# Enhanced molecular doping for high conductivity in polymers with volume freed for dopants

Hui Li, $^{\dagger, \dagger}$  Mallory E. DeCoster, $^{\S}$  Chen Ming, $^{\dagger}$  Mengdi Wang, $^{\dagger}$  Yanling Chen, $^{\dagger}$  Patrick E. Hopkins, $^{\S}$  Lidong Chen $^{*, \dagger, \perp}$  and Howard E. Katz $^{*, \dagger}$ 

†State Key Laboratory of High Performance Ceramics and Superfine Microstructures, Shanghai Institute of Ceramics, Chinese Academy of Sciences, Shanghai 200050, China

<sup>‡</sup>Department of Materials Science and Engineering, Johns Hopkins University, 3400 North Charles Street, Baltimore, Maryland 21218, United States

§Department of Mechanical and Aerospace Engineering, University of Virginia, Charlottesville, Virginia 22904, United States

<sup>1</sup>Center of Materials Science and Optoelectronics Engineering, University of Chinese Academy of Sciences, Beijing 100049, China

**ABSTRACT:** We present two new polythiophene isomers, PQTC16-TT and PQTSC16-TT, with more separation and lower side chain density on the backbone compared with the typical polythiophenes, such as PQT(S)12 and PBTTT(S)12. The introduction of spacer subunits to separate the side chains improves the accommodation of dopant molecules close to the polymer backbone. Therefore, the lamellar structure and  $\pi$ - $\pi$  stacking of polymers were negligibly disturbed by dopants; in fact, improved ordering and closer  $\pi$ -stacking were observed after chemical doping.

Furthermore, the doping efficiency is significantly enhanced and the electrical conductivity is improved up to 330 S cm<sup>-1</sup>, still maintained at 200 S cm<sup>-1</sup> at higher doping concentration, for the combination of PQTSC16-TT/NOBF4. We investigate how charge transfer is affected by the geometry of the dopant with respect to the polymer repeat unit. It is shown that the sulfurs in the side chains act as binding sites for dopants, resulting in higher thermal and environmental stability of alkylthio-substituted polymers upon doping.

## **INTRODUCTION**

Polymer semiconductors can be easily processed into thin films and are promising for the realization of flexible electronics. The use of polymer semiconductors as conductive layer in organic thermoelectric (TE) devices has attracted increased attention in recent years. 1, 2 The TE performance of a material is defined as a dimensionless figure of merit,  $ZT = S^2 \sigma T / \kappa$ , where S is the Seebeck coefficient,  $\sigma$  is electrical conductivity,  $\kappa$  is thermal conductivity, and T is absolute temperature. Chemical doping, accompanying the charge transfer from the highest occupied molecular orbital (HOMO) of the polymer to the lowest unoccupied molecular orbital (LUMO) of the dopant molecules (p-type doping),<sup>3, 4</sup> has become a popular approach to control the electrical properties of polymer semiconductors.<sup>5, 6</sup> However, low efficiency of doping remains a challenge for obtaining high thermoelectric performance because the dopants usually interrupt the charge transport of pristine polymers and tend to aggregate, resulting in a low electrical conductivity<sup>7</sup> and thus a low ZT. Furthermore, a dramatic drop of electrical conductivity usually happens at high doping level with poor film quality. 8 There have been several technical approaches to avoid this issue. One major strategy was to immerse a polymer film into a dopant solution for an extended time to ensure the intrinsic packing of the film would not be damaged. 9-11 Tang et al. reported a power factor (PF =  $S^2\sigma$ ) of 19  $\mu$ W m<sup>-1</sup> K<sup>-2</sup> was obtained for  $\gamma$  oxygen-substitution on the side chains of poly(3-hexylthiophene) (P3HT) analogue by immersing films into FeCl<sub>3</sub> solution.<sup>12</sup> Evaporating dopant into the polymer film under ultra-high vacuum is another technique to pursue high electrical conductivity.<sup>13-16</sup> Thus, it has been demonstrated that the electrical conductivity of poly[2,5-bis(3-tetradecylthiophen-2-yl)thieno[3,2-b]thiophene] (PBTTT-C14) can be enhanced to up to 250 S cm<sup>-1</sup> when doped by 2,3,5,6-tetrafluoro-7,7,8,8-tetracyanoquinodimethane (F4TCNQ).<sup>17</sup> Additionally, Schwartz et al. proposed a sequential doping method where the dopant solution was spin-coated onto the polymer film. The electrical conductivity of P3HT film was improved to 9.1 S cm<sup>-1</sup>.<sup>18, 19</sup> This method was also successfully applied to other polymers.<sup>20-23</sup> All these strategies aim at avoiding or weakening the interference of dopant to the packing of polymer during the doping process, but the complicated and strict experimental conditions, such as multi-step processes, limited film thicknesses, and high vacuum, are required. The molecular doping by single solution processing of polymer/dopant mixture is a simple method, but there have been few reports achieving high electrical conductivity over 100 S cm<sup>-1</sup>.<sup>4, 24</sup>

To improve the electrical conductivity of co-processed films from solution and reveal the doping mechanism, much attention was recently paid on the modification of polymer backbone and side chains to control the doping efficiency. Backbone regiochemistry<sup>25</sup> and the polaron delocalization length<sup>26</sup> of the n-type polymers in the doped phase were linked to the electrical conductivity. Important progress was also made for the development of the side chains. For instance, using polar oligoethylene glycol as side chains<sup>4, 7, 27-29</sup> favors the dispersion of dopant into the polymer matrix and significantly improves the electrical conductivity. A 200-fold enhancement of electrical conductivity was achieved by Koster for an N2200 derivative by using this strategy.<sup>28</sup> Additionally, the length of the alkyl side chain has influence on the doping mechanism.<sup>30, 31</sup> Jang

et al. reported that the existence of long side chains of the D-A polymer allowed retaining good solubility and adding large amounts of F4TCNQ would not severely disturb the polymer ordering.<sup>30</sup> Development of new soluble dopants would be another approach for solution processed films with high electrical conductivity.<sup>8, 32-34</sup> Pei et al. proposed that, for ordered n-type polymers, proper shape of the counterion will cause less perturbation of the film microstructures.<sup>35</sup> Schwartz et al. provided an example that, by utilizing a substituted boron cluster as a molecular dopant to shield the polaron from the anion, the electrical conductivities and polaron mobilities of P3HT was an order of magnitude higher than films doped with F4TCNQ.<sup>36</sup> Graham et al. investigated the influence of dopant size on doping efficiency and demonstrated the bulky dopant will weaken the coulomb interaction between the polaron and dopant anion, but also disrupt the crystallinity of polymers at high loadings.<sup>37</sup>

From the viewpoint of polymer backbone and side chain, in our previous work, we modified the poly(bisdodecylquaterthiophene) (PQT12) by inserting EDOT groups into backbone and/or sulfur into the side chains and obtained high conductivity of 350 S cm<sup>-1</sup> via single-solution processing, and the conductivity dramatically decreased to 80 S cm<sup>-1</sup> at molar ratio of 1.<sup>24</sup> That means the high conductivity is limited by a specific doping level. To further address the challenge of high conductivity by facile solution processing, we propose that the influence of dopant on polymer packing is predominantly via two factors: (i) large density of insulating alkyl chains around the backbones lead to disordered stacking of the backbones and hamper the dopant being close to the backbone; (ii) binding sites close to the backbone could enhance the interaction between repeat unit and dopant. Therefore, providing enough space for dopant to fit comfortably into the polymer morphology could be a valuable approach for effective doping. In this article, we will focus on the synthetic modification of polymer semiconductors by significantly increasing the space for dopant

to occupy without the perturbation of film microstructure. To prove the role of "spacer" on polymer backbone and the matching of dopant-polymer structure, we include examples of doped polymers with large molar ratio (1 to 1 for dopant to repeat unit).

The polymers chosen for this study are displayed in Figure 1a. Two new polymers, PQTC16-TT and PQTSC16-TT, with more widely spaced insulating side chains on the backbone are synthesized. The key points of our design are: 1) The extra thienothiophene units act as spacers that make the polymers different from the standard polymer, PQT polymers; 2) longer side chains (C16) are chosen for better solubility and may also increase volumes for dopants along the lamellar directions; 3) Different from the structure of PBTTT in which the alkyl chain is adjacent to the thienothiophene, the alkyl chains in the new polymers are adjacent to bithiophene to reduce the steric interactions; 4) Sulfur atoms are directly grafted onto the thiophene ring. The existence of sulfur will influence the polymer packing, but also importantly will decrease the polymer ionization potentials. High doping efficiency was observed in UV-Vis-NIR absorption spectra compared with PQT(S) polymers or PBTTT(S) polymers. The packing of new polymers was not disturbed even under high doping level (Figure 1b) determined by grazing incidence wide-angle X-ray scattering (GIWAXS), while significant self-aggregation of dopants was observed in F4TCNQ-doped PQT(S)12 or F4TCNQ-doped PBTTT(S)C12. The carrier mobilities of these two new longer-side-chain polymers are relatively lower  $(0.008 \sim 0.01 \text{ cm}^2 \text{ V}^{-1} \text{ s}^{-1})$  compared with the shorter-side-chain counterparts, PQT(S)12 (0.03 cm<sup>2</sup> V<sup>-1</sup> s<sup>-1</sup> for PQT12 and 0.01 cm<sup>2</sup> V<sup>-1</sup> s<sup>-1</sup> for PQTS12, respectively) or PBTTT(S)C12 (0.13 cm $^2$  V $^{-1}$  s $^{-1}$  for PBTTTC12 and 0.01 cm $^2$  V $^{-1}$  s $^{-1}$  for PBTTTSC12, respectively). However, doped by F4TCNQ, the highest electrical conductivity up to 55 S cm<sup>-1</sup> was obtained for PQTSC16-TT, which is among the highest values for single solutiondeposited thiophene polymers mentioned above. Doped by a smaller and stronger dopant, NOBF4,

more charge transfer was stimulated and a higher electrical conductivity up to 330 S cm<sup>-1</sup> was achieved for PQTSC16-TT. The conductivity could be still maintained at 200 S cm<sup>-1</sup> even at higher doping concentration. Although the Seebeck coefficient was not optimized, a *ZT* value of 0.012 was obtained. It was demonstrated that the increased space along the polymer backbone provided more possible geometries for dopant close to the polymer backbone, also associated with low activation energy for charge transport. Furthermore, we observed that the presence of sulfurs in the side chains acting as binding sites for dopants not only results in higher electrical conductivity but also higher thermal and environmental stability of doped films.

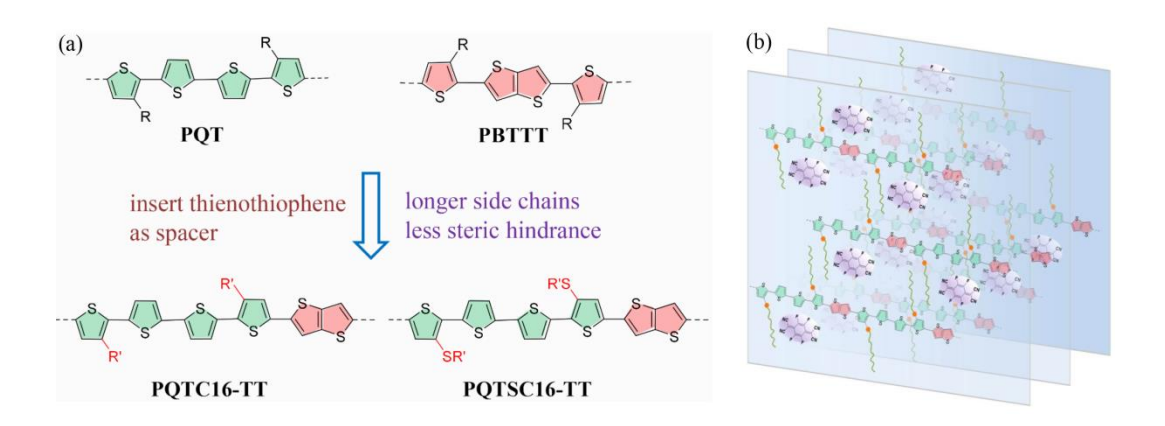


**Figure 1.** (a) Design strategies of PQT-TT polymers. The green and red pentagons highlight the QT unit and thienothiophene unit, respectively. The red side chain highlights the orientation to thienothiophene of side chains; (b) A proposed schematic diagram dopants in polymer chains (The orange dots represent sulfur atoms in the side chains and F4TCNQ represents dopant).

#### RESULTS AND DISCUSSION

# Synthesis and Characterization of PQT(S)C16-TT Polymers

The synthetic routes to PQTC16-TT and PQTSC16-TT are shown in Figure S1. The polymers were obtained by typical Stille polymerization with high yield. C16 was used as side chains to ensure the solubility of polymers in halogenated solvents, such as hot chloroform and chlorobenzene. The molecular weights of polymers were evaluated by MALDI-TOF<sup>7</sup> (Figure S2) and S3). PQTC16-TT exhibits a maximum length of n = 111 repeating units while PQTSC16-TT has a maximum length of n = 113 repeating units, which means the molecular weights of these two polymer are close. The thermogravimetric analysis (TGA) in Figure S4 indicates that two polymers exhibit good thermal stability above 320 °C and PQTC16-TT shows higher decomposition temperature. PQT(S)C16-TT polymers exhibit no obvious thermal transition by differential scanning calorimetry (DSC) upon heating to 300 °C (Figure S5). This is different from POT(S)12 or PBTTT analogy in which backbone and/or side-chain melting can be observed. 24, 38 The electrochemical properties of the PQT(S)C16-TT polymers were investigated by cyclic voltammetry (Figure S6). We compared the energy levels of the PQT(S)C16-TT polymers with PQT(S)12 and PBTTT(S)C12<sup>38, 39</sup> in Figure S7 and we found that the HOMO level of POTC16-TT (-5.19 eV) and PQTSC16-TT (-5.08 eV) is much closer to the HOMO level of PBTTTC12 (-5.20 eV) and PBTTTSC12 (-5.10 eV), respectively. The charge carrier mobilities of PQT(S)C16-TT polymers were tested in field-effect transistor (FET) devices with top-contact/bottom-gate device architecture (Figure S8). The mobilities of these two polymers are similar ( $\sim 0.01~\text{cm}^2~\text{V}^{\text{-1}}$ s<sup>-1</sup>). We propose that the longer alkyl chains (C16) of the two polymers impact the carrier transport and the mobility is lower than that of PBTTTC12 (0.13 cm<sup>2</sup> V<sup>-1</sup> s<sup>-1</sup>) and PQT12 (0.03 cm<sup>2</sup> V<sup>-1</sup> s<sup>-1</sup>).

## **UV-vis-NIR Spectroscopy of Pristine Polymers and Doped Polymers**

The thickness-normalized absorption spectra of pristine polymers and doped polymers are shown in Figure 2 to depict the doping process. For all combinations below, molar ratio of 1 to 1 is typically used for dopant to repeat unit, or as specifically mentioned. The existence of sulfur in the side chains of pure PQTSC16-TT results in a bathochromic shift of the  $\pi$ - $\pi$ \* absorption peak and close packing in the film indicated by a significant shoulder peak at 603 nm. A similar phenomenon was also observed in pure PQTS12 film.<sup>24</sup> Upon doping with F4TCNQ, the subgap absorption (750 nm ~ 2000 nm), assigned to the absorption of (bi)polaron of polymer, grows at the expense of the  $\pi$ - $\pi$ \* absorption of the neutral polymer. The absorption peaks of F4TCNQ anion locate at 416 nm, 777 nm and 882 nm, which are overlapped with the oxidized polymer, meaning the existence of integer charge transfer between polymer and dopant. 4, 40, 41 In Figure S9, with more F4TCNQ added, the intensities of its anion peaks and polymer (bi)polaron peaks gradually increase from molar ratio of 0.33, 0.65 to 1.0, indicating the increased doping efficiency. The spectral features due to charge transfer are more pronounced in PQTSC16-TT/F4TCNQ, as are the decrease in absorption of neutral polymer, than those of PQTC16-TT/F4TCNQ at the same doping ratio. This indicates the higher doping efficiency for alkylthio-substituted polymers. When the molar ratio is higher than 1.0, the increase of anion or (bi)polaron peaks becomes negligible and the absorption of the neutral polymer becomes a little strong probably attributed to the aggregation of F4TCNQ itself in very high doping ratio. Compared with F4TCNQ-doped polymers, NOF4doped polymers show stronger (bi)polaron absorption in the range of 1200 nm ~ 2000 nm for PQTC16-TT and PQTSC16-TT, respectively. That indicates the higher doping efficiency in NOBF4-doped polymers because of the stronger oxidizability and lower LUMO level of NOBF4 (the calculation of the LUMO level can be found in SI). To verify the influence of spacer on doping

level in our new polymers, we further compare the absorption spectra of F4TCNQ-doped PQT(S)C16-TT with typical polymers, PQT(S)12 and PBTTT(S)12, at molar ratio of 1 (Figure 3). It is significant that the absorption intensity of F4TCNQ anion is much stronger for PQTC(S)16-TT/F4TCNQ than those of doped PQT(S)12 and doped PBTTT(S)12. Moreover, F4TCNQ-doped sulfur-substituted polymers shows stronger anion intensities than those of polymers without sulfur in the side chains. In particular, the neutral absorption of polymer almost disappears in PQTSC16-TT/F4TCNQ film. Considering the similar HOMO levels for PQT(S)C16-TT and PBTTT(S)C12, we propose that the occurrence of integer charge transfer is not mainly determined by the driving force from energy level difference between polymer and dopant. The higher doping efficiency is most likely attributed to the increased spacing and intimate contact between F4TCNQ molecules and polymer backbone in PQT(S)C16-TT film.

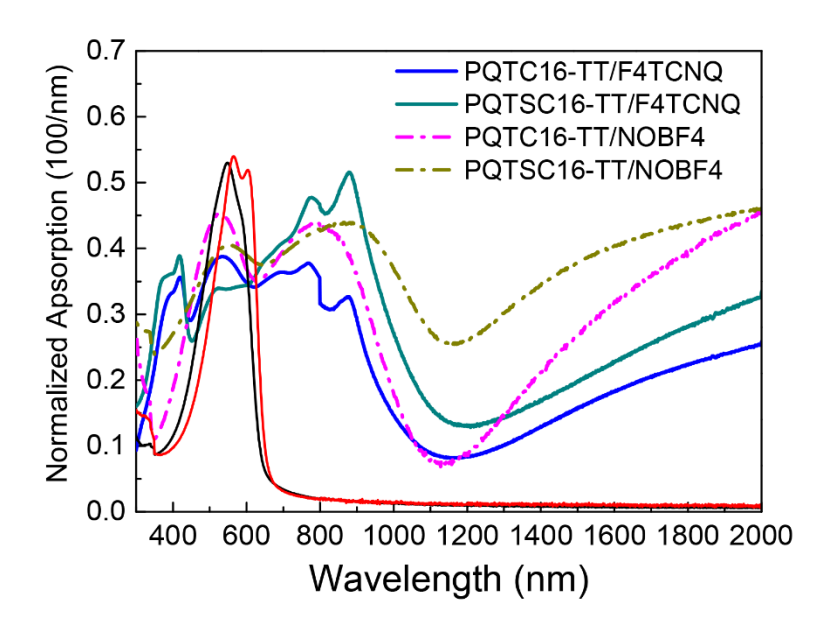


**Figure 2.** Thickness-normalized UV-vis-NIR absorption spectra of doped polymers (molar ratio of 1:1).

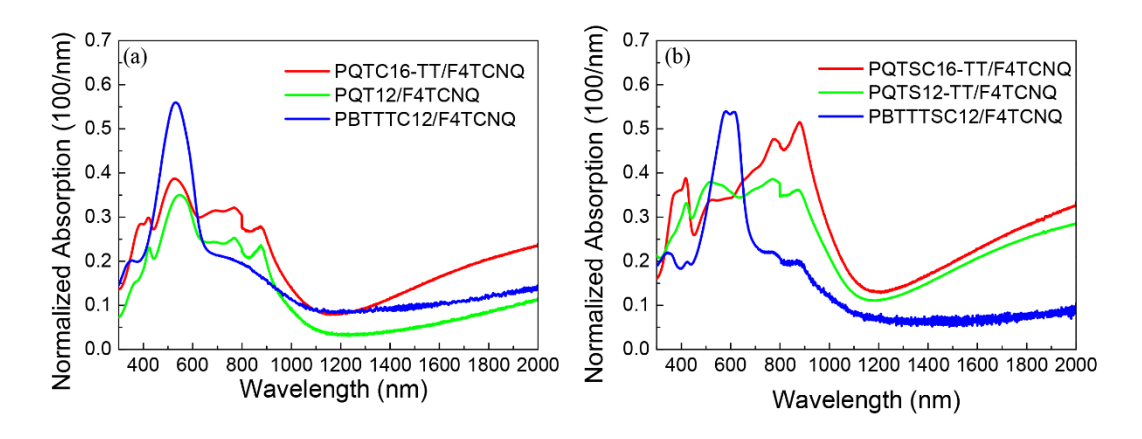


**Figure 3.** Thickness-normalized UV-vis-NIR absorption spectra of F4TCNQ-doped polymers with molar ratio of 1:1.

# Thermoelectric Measurements of PQT(S)C16-TT Polymers

The electrical conductivities of the doped polymers were measured by a four-point-probe method as before. <sup>42</sup> All films were fabricated by a single solution-deposited method. The preparation details can be found in the Supporting Information. In Figure 4, doping with different ratios of F4TCNQ, PQTSC16-TT always shows higher electrical conductivity than that of PQTC16-TT. For a molar ratio of 1, PQTC16-TT and PQTSC16-TT show the highest electrical conductivity up to 15 S cm<sup>-1</sup> and 55 S cm<sup>-1</sup>, respectively. Worth noting is that the electrical conductivity did not significantly decrease with more F4TCNQ being added. The electrical conductivity is still maintained at 40 S cm<sup>-1</sup> for a molar ratio of 3.5 (3.5 F4TCNQ for one repeat unit) for PQTSC16-TT/F4TCNQ. We propose that the high electrical conductivity at this dopant concentration can be attributed to there being sufficient space along the polymer backbone due to the introduction of thienothiophene units, and a driving force for dopant to be located in each space near the polymer backbones where it can be accommodated, even though some of the dopant may be in a separate phase. Doping with the stronger oxidant NOBF4, PQTSC16-TT shows the highest electrical

conductivity up to 330 S cm<sup>-1</sup>, while PQTC16-TT shows the highest electrical conductivity of 39 S cm<sup>-1</sup> at molar ratio of 1. Compared with F4TCNQ-doped polymers, the electrical conductivity significantly decreases with adding excess NOBF4, which means the morphology or charge transport paths can be easily impeded by the tetrahedral BF4 anion. This is also observed in the doping process of NOBF4-doped PQTS12. We also fabricated TE devices by spin coating the doped solution on the substrates. We observed that different processing methods do not change the trend of conductivity of these four combinations; that is, doped PQTSC16-TT films show higher conductivity and PQTSC16-TT /NOBF4 has the highest conductivity. This indicates that the efficient doping is mainly dominated by structures and processes at the molecular level.

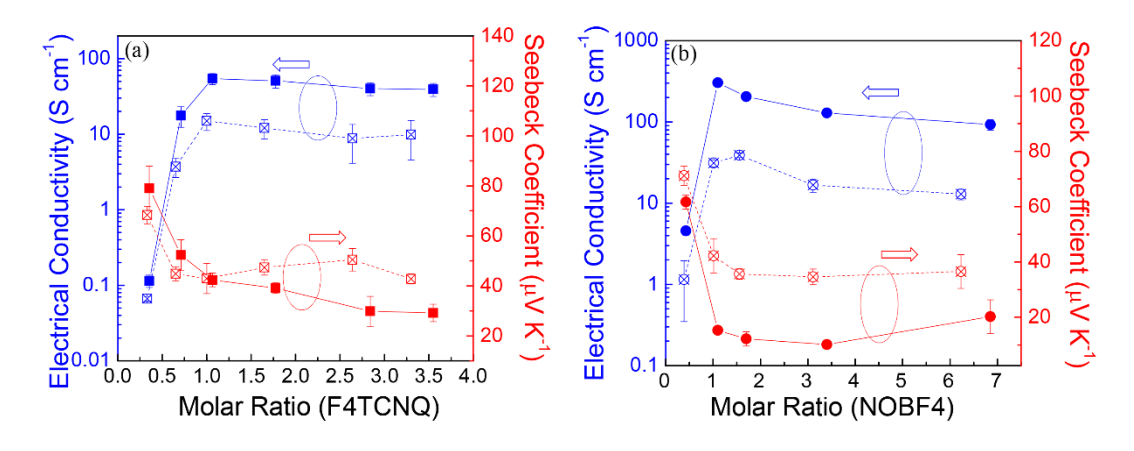


**Figure 4**. Electrical conductivity and Seebeck coefficient of F4TCNQ-doped polymers (a) and NOBF4-doped polymers (b) with varied molar ratio of dopant to polymer repeat unit. (PQTC16-TT: open symbols, PQTSC16-TT: close symbols)

We compared the electrical conductivities of PQT(S)C16-TT with PQT(S)12 and PBTTT(S)C12 under the same doping condition (molar ratio of 1) in Figure S10. It is observed that PQTC16-TT and PQTSC16-TT show outstanding conductivity among these polymers. The conductivity of PQTSC16-TT/F4TCNQ is 1.7 times higher than the conductivity of PQTS12/F4TCNQ and 7 times

higher than that of PBTTTS12/F4TCNQ processed in single solution, while the conductivity of PQTSC16-TT/NOBF4 is 2 times higher than the conductivity of PQTS12/NOBF4 and 100 times higher than that of PBTTTS12/NOBF4, indicating a benefit from our design strategy. Overall, the polymers with sulfur in the side chains exhibit higher electrical conductivity than those of their analogies without sulfur in the side chains. Also, the conductivities of PBTTT(S)C12 doped by NOBF4 or F4TCNQ are clearly lower, suggesting that the steric hindrance from F4TCNQ and BF4 anion profoundly disturb the packing of pristine PBTTT.

The Seebeck coefficients of PQT(S)C16-TT polymers change in opposite directions when the electrical conductivities change (Figure 4), as expected from such paired characterizations of the same transport mechanism. Also, the relationship between the conductivities and Seebeck coefficients fit well with the empirical model developed by the Chabinyc group. 13 To estimate the figure of merit, ZT, the thermal conductivities of doped films with molar ratio of 1 were measured using time domain thermoreflectance (TDTR) and optical pump-probe thermometry technique. 43-<sup>44</sup> Due to the challenge of measuring the in-plane thermal conductivity  $(\kappa_{//})$  for polymer films, we simply obtained the thermal conductivity along the out-of-plane direction ( $\kappa_{\perp}$ ). Nevertheless, the significant amorphous and non-oriented fraction of the polymer film, in contrast to more crystalline materials, decreases the anisotropy of the thermal conductivity. The schematic of the TDTR setup is shown in Figure S11 and the details about the measurement and analysis are discussed further in the Supporting Information. We found that F4TCNQ-doped or NOBF4-doped POT(S)C16-TT show very low thermal conductivity around 0.21 W m<sup>-1</sup> K<sup>-1</sup> along the out-of-plane direction (Figure S12 and Table S1). An increase in the thermal conductivity is observed as the polymers are doped by F4TCNQ at higher molar ratios (Figure S13). For F4TCNQ-doped PQTSC16-TT, the ZT value is 0.016 while the ZT value is 0.012 for NOBF4-doped PQTSC16-TT

based on the measured out-of-plane thermal conductivity, which is higher than the performance of PQTS12/NOBF4 (ZT = 0.0051) in our previous work.<sup>24</sup> This analysis was done largely to illustrate the relative contribution that improved doping effectiveness increased desired charge transport in structurally related polymers.

## **Crystallinity and Molecular Packing of Films**

To further study the impact of dopants on the microstructure of polymer films in detail, we performed GIWAXS measurements (Figure 5 and Figure S14). All films were annealed at 60 °C for 30 min in glove box before testing. The neat film of PQTC16-TT shows a weak peak along the out-of-plane direction and no peak was observed along the in-plane direction, indicating limited crystallinity. For the neat PQTSC16-TT film, the peaks observed both in the out-of-plane pattern and in-plane pattern indicate that face-on and edge-on configurations simultaneously exist. After doping, all doped films notably exhibit multiple order scattering features along the out-of-plane direction while the  $\pi$ - $\pi$  stacking becomes much clearer, indicating ordered structures appear upon doping. The lamellar distance slightly increases in F4TCNQ-doped PQTC16-TT and NOBF4doped PQTC16-TT film ( $\Delta \approx 2.5 \text{ Å}$ ) (Table S2). However, we found that the lamellar distance is almost unchanged comparing neat PQTSC16-TT film with F4TCNQ-doped PQTSC16-TT film (Δ = 0.77 Å) and NOBF4-doped PQTC16-TT film ( $\Delta$  = 0.12 Å). These results indicate that the excess space, together with sulfur atoms in the side chains, are beneficial for intercalation of planar or relatively small dopants in the alkyl side-chain region and sulfur atoms act as binding sites for dopants. Different from the change of the lamellar structure, the  $\pi$ - $\pi$  stacking distance significantly decreases after doping. For PQTC16-TT film, the  $\pi$ - $\pi$  interaction is stronger for NOBF4-doped PQTC16-TT film (3.43 Å) than that for F4TCNQ-doped film (3.45 Å), and for PQTSC16-TT, the  $\pi$ - $\pi$  stacking distance decreases from 3.62 Å to 3.44 Å and to 3.40 Å for neat film, F4TCNQ-doped film and NOBF4-doped film, respectively. The intense  $\pi$ - $\pi$  interaction is most likely responsible for the enhanced electrical conductivity. No peaks from F4TCNQ aggregation are observed for PQTC16-TT/F4TCNQ and PQTSC16-TT/F4TCNQ at molar ratio of 1 to 1 for dopant to repeat unit. In contrast, the self-aggregation of F4TCNQ (large arcing diffractions around  $q_z = 0.75$  Å<sup>-1</sup> in Figure S15) obviously appears in F4TCNQ-doped PQT(S)12 and F4TCNQ-doped PBTTT(S)C12 under the same doping condition. Even for molar ratio of 0.5 for F4TCNQ to repeat unit, the diffraction of F4TCNQ still be observed in F4TCNQ-doped PQT(S)12 film.<sup>24</sup> This indicates the large density of alkyl chains restrains the intercalation of dopants into the lamellar structures of polymers.

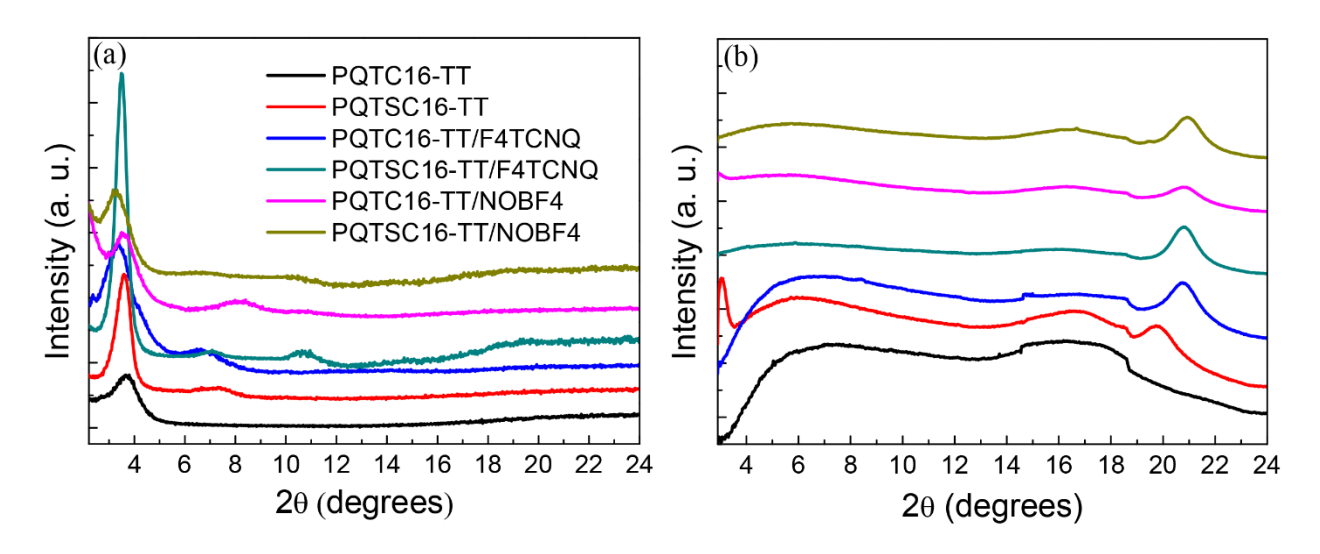


**Figure 5.** (a) Out-of-plane pattern and (b) in-plane pattern of pure polymers and doped polymers. (The molar ratio of dopant to repeat unit is 1 to 1; out-of-plane curves were tested by XRD with  $\lambda$  of 1.54 Å and in-plane curves were extracted from 2D-GIWAXS image with  $\lambda$  of 1.24 Å)

## **Temperature-dependent Thermoelectric Properties**

To understand the charge transport in doped polymers, the temperature-dependent electrical conductivities and Seebeck coefficients were measured. In Figure 6, the electrical conductivities increase in all formulations as the temperature increases while Seebeck coefficients are weakly dependent on temperature (Figure S16), indicating that Mott polaron model is probably suitable for describing the thermally activated charge transport. 45-48 We also measured the temperaturedependent electrical conductivities of PQT(S)12 and PBTTT(S)C12 (Figure S17). The thermal activation energy  $(E_A)$  related to the energy barrier for charge transport can be obtained according to the equation:  $\sigma = \sigma_i \exp(-E_A/k_BT)$ , where  $\sigma_i$  is a temperature-independent prefactor and  $k_B$  is Boltzmann constant. To avoid undue interferences from thermally induced dedoping of films, the temperature ranges (298 ~ 320 K for NOBF4 doped films and 298 ~ 340 K for F4TCNQ doped films, respectively) where electrical conductivity is proportional to temperature, were selected to calculate  $E_A$  (ln $\sigma$  versus 1/T). Cooling from these temperatures resulted in immediate conductivity decreases, confirming that the conductivity increases were not due to irreversible changes. The relationship of  $E_A$  and electrical conductivity of all doped films are shown in Figure 7. It is found that all films doped by NOBF4 show lower  $E_A$  than those of films doped by F4TCNQ, associated with higher electrical conductivities being obtained for the former films. Moreover, NOBF4-doped polymers with sulfur in the side chains show much lower  $E_A$  and lower Seebeck coefficients (~ 20 μV K<sup>-1</sup>) among all these combinations. This indicates that the activation energies may include contributions from barriers between high-conductivity domains, rather than being entirely from the thermal excitation energy between Fermi and transport levels.<sup>35, 44</sup> For F4TCNQ doped films, higher  $E_A$  was observed for the polymers with sulfur in the side chains, which could be associated with the lower carrier mobility of sulfur-substituted polymers than those of polymers without sulfur in the side chains.<sup>24, 42</sup> Moreover, PQTSC16-TT/F4TCNQ shows lower  $E_A$  than that of PQTS12/F4TCNQ or PBTTTSC12/F4TCNQ in which the morphology was perturbed by the self-aggregation of dopants and thus the barrier for charge transport was increased. Therefore, low activation energy and high electrical conductivity of our new polymers could be the synergistic effect of charge transfer efficiency and charge transport path ascribed to the polymer structure with freed volume for the dopants.

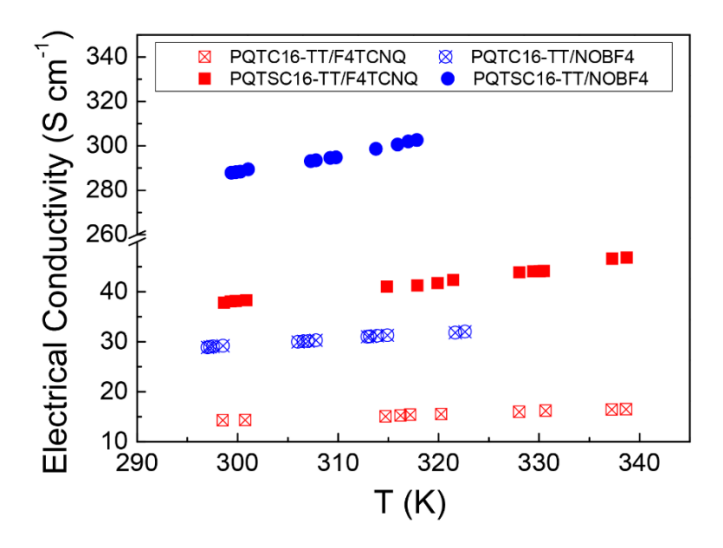
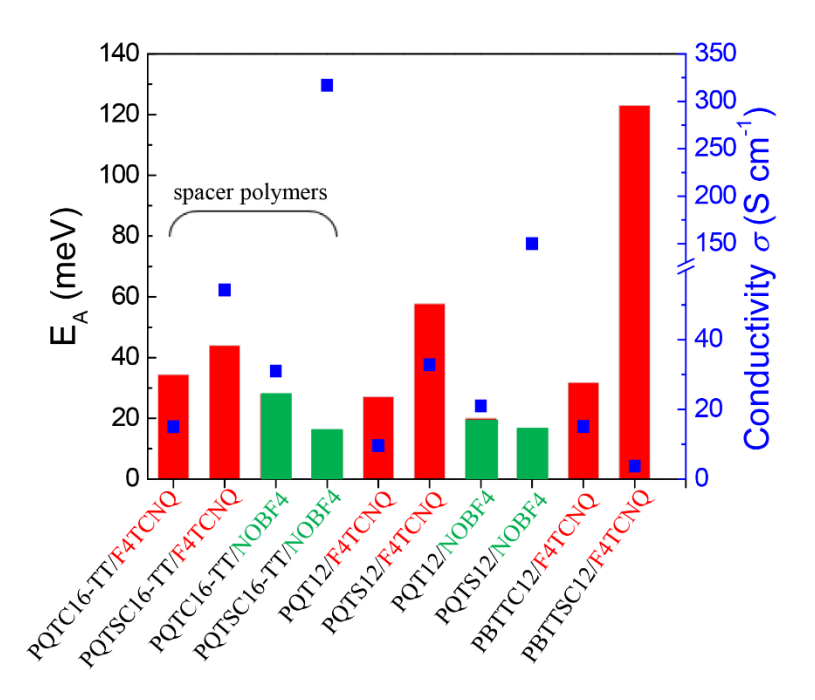


Figure 6. Temperature-dependent electrical conductivities at molar ratio of 1.



**Figure 7.** The comparison of activation energies of all formulations with respect to their electrical conductivities (molar ratio is 1). All bars describe activation energy ( $E_A$ ) and blue squares describe electrical conductivity ( $\sigma$ ). Red bars represent the  $E_A$  of F4TCNQ-doped polymers; Green bars represent the  $E_A$  of NOBF4-doped polymers. (PBTTTC12/NOBF4 and PBTTTSC12/NOBF4 were skipped due to insufficient data points between 300 K and 340 K).

## Thermal and Environmental Stability of Thermoelectric Devices

In Figure 8 and Figure S17, the dedoping occurs for all films at higher temperature which is the commonly observed behavior for disordered thiophene polymers. However, the PQTSC16-TT shows higher dedoping temperature both in F4TCNQ-doped film and NOBF4-doped film. For example, the dedoping temperature increases 40 °C in PQTSC16-TT/F4TCNQ compared with PQTC16-TT/F4TCNQ film and increases 20 °C for PQTSC16-TT/NOBF4 compared with PQTC16-TT/NOBF4. The same phenomenon was observed in doped PQ(S)T12 and doped PBTTT(S)C12 (Figure S17), in which the polymers with sulfur in the side chains show higher

thermal stability. This observation can be related to a reported thermal stability up to 150 °C for F4TCNQ-doped polythiophene functionalized by oligo ethylene glycol.<sup>27</sup> In the present work, even though only two sulfur atoms exist in one repeat unit of polymer, the thermal stability can increase to 110 °C. The existence of sulfur in the side chains also influences the stability of devices in air. As shown in Figure S18, the degradation of conductivity was significantly restrained for doped PQTSC16-TT compared with doped PQTC16-TT. For instance, the conductivity decreases about 66% for PQTSC16-TT/F4TCNQ while almost complete degeneration happens for PQTC16-TT/F4TCNQ, strored in moist air (~ 65% humidity) for three months. Also, the conductivity decreases 45% for PQTSC16-TT/NOBF4 and 95% for PQTC16-TT/NOBF4, respectively, stored in moist air for 20 days. The sulfur atoms in the side chains could serve as binding sites for dopants. Additional evidence for this interaction was obtained from Fourier transform infrared spectroscopy (FTIR) as shown in Figure S19. It is found that the peak at 720 cm<sup>-1</sup> originating from the C-S bond becomes down-shifted after doping, illustrating a likely effect of dopant on the C-S bond. The existence of sulfur atoms in the side chains makes the device more resistant to temperature, water and oxgen, which is critical for designing new conductive polymers for their practical applications.

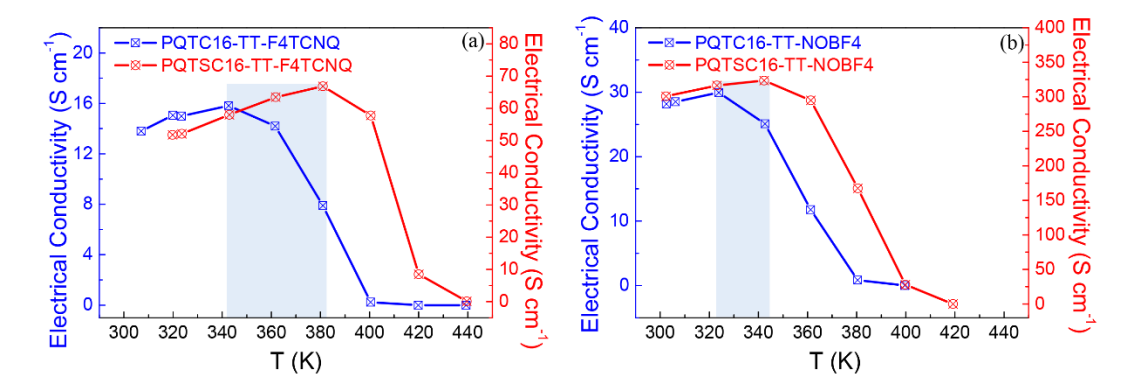


**Figure 8.** Temperature-dependent electrical conductivity of PQTC16-TT and PQTSC16-TT doped with F4TCNQ (a) and NOBF4 (b), respectively. The shaded region indicates increased stability of doped PQTSC16-TT formulations.

### **DFT Calculations**

According to the results of GIWAXS, F4TCNQ or NOBF4 tends to intercalate into the lamellar structure of polymer rather than forming a complex where it is co-facially aligned with the polymer backbone as was found in F4TCNQ- doped PBTTT.<sup>50</sup> Here, different geometrical configurations were tested by changing the position of F4TCNQ along the repeat unit of PQTC16-TT. The optimized geometry is F4TCNQ being close to bithiophene or thienothiophene, which shows much lower total energy (Figure S20 and Table S3). This demonstrates that the spacer from thienothiophene did provide more positions for F4TCNQ molecule closer to the polymer backbone. On the other hand, this is consistent with the experimental results that electrical conductivity did not significantly decrease even with molar ratio of 2 (Figure 3). The calculation also proves that sulfur in the side chain can stabilize the geometry for F4TCNQ-doped PQTSC16-TT with larger  $\Delta E$  ( $\Delta E = E_{\text{dopant}} + E_{\text{polymer chain}} - E_{\text{complex}}$ ) compared with PQTC16-TT/F4TCNQ (Figure S21), with a larger amount of transferred charge (0.75 e) compared with PQTC16-TT/F4TCNQ (0.69 e). This indicates that sulfur atom acts as a binding site and agrees well with the better thermal stability of doped PQTSC16-TT/F4TCNQ. For NOBF4, these two combination show similar  $\Delta E$  and the transferred charge is close to 1 (0.96 e). This can be ascribed to the strong oxidizability of NOBF4 capturing the electron from the polymer without selectivity. Although similar thermal stability of the doped films is observed for PQTC16-TT/NOBF4 and PQTSC16-TT/NOBF4, the existence of sulfur atoms in side chains apparently slows the degradation of the

latter composition from water/oxygen. Therefore, this type of side chain modification could be an important strategy for designing TE polymers with high environmental stability.

## **CONCLUSIONS**

In summary, we have demonstrated that high doping efficiency and large amount of charge transfer can be carried out by introducing much spacer in polymer backbone via experimental results and DFT calculations. Due to the accommodation of dopant molecules close to the polymer backbone, low activation energy ascribed to the effective charge transfer and ordering charge transport path leads to a high electrical conductivity of 330 S cm<sup>-1</sup> and a ZT value of 0.012 for NOBF4-doped polymer. It is also evident that the existence of sulfur, providing large driving force for charge transfer, acts as binding sites for dopants and lead to higher thermal and environmental stability of doped film. Based on these findings, we proposed that not only providing sufficient volume for dopant in polymer network, but also simultaneously optimizing the structure of the side chains can improve the efficiency of charge transfer.

## ASSOCIATED CONTENT

## **Supporting Information**

Details of instruments, device fabrication and synthesis of monomers and polymers, NMR, TGA, DSC characterization, 2D-GIWAXS data, thermal conductivity, DFT calculation and other data (PDF).

#### AUTHOR INFORMATION

# **Corresponding Author**

\* E-mail: cld@mail.sic.ac.cn; hekatz@jhu.edu

#### Notes

The authors declare no competing financial interest.

## **ACKNOWLEDGMENT**

Work at Johns Hopkins University, including polymer synthesis, doping, and conductivity studies, was supported by the National Science Foundation, Division of Chemistry, Grant Number 1708245. H. Li acknowledges additional financial support from the Shanghai Sailing Program for work performed at Shanghai Institute of Ceramics. We thank Jie Xiao for DSC measurements. The authors acknowledge beamtime provided by beamline BL14B1 (Shanghai Synchrotron Radiation Facility).

## **REFERENCES**

- (1) Kroon, R.; Mengistie, D. A.; Kiefer, D.; Hynynen, J.; Ryan, J. D.; Yu, L.; Müller, C. Thermoelectric plastics: from design to synthesis, processing and structure–property relationships. *Chem. Soc. Rev.* **2016**, *45*, 6147-6164.
- (2) Russ, B.; Glaudell, A.; Urban, J. J.; Chabinyc, M. L.; Segalman, R. A. Organic thermoelectric materials for energy harvesting and temperature control. *Nat. Rev. Mater.* **2016**, *1*, 16050.
- (3) Karpov, Y.; Erdmann, T.; Raguzin, I.; Al-Hussein, M.; Binner, M.; Lappan, U.; Stamm, M.; Gerasimov, K. L.; Beryozkina, T.; Bakulev, V.; Anokhin, D. V.; Ivanov, D. A.; Günther, F.; Gemming, S.; Seifert, G.; Voit, B.; Di Pietro, R.; Kiriy, A. High Conductivity in Molecularly p-

- Doped Diketopyrrolopyrrole-Based Polymer: The Impact of a High Dopant Strength and Good Structural Order. *Adv. Mater.* **2016**, *28*, 6003.
- (4) Kiefer, D.; Kroon, R.; Hofmann, A. I.; Sun, H.; Liu, X.; Giovannitti, A.; Stegerer, D.; Cano, A.; Hynynen, J.; Yu, L.; Zhang, Y.; Nai, D.; Harrelson, T. F.; Sommer, M.; Moulé, A. J.; Kemerink, M.; Marder, S. R.; McCulloch, I.; Fahlman, M.; Fabiano, S.; Müller, C. Double doping of conjugated polymers with monomer molecular dopants. *Nat. Mater.* **2019**, *18*, 149-155.
- (5) Hu, Y.; Rengert, Z. D.; McDowell, C.; Ford, M. J.; Wang, M.; Karki, A.; Lill, A. T.; Bazan, G. C.; Nguyen, T.-Q. Doping Polymer Semiconductors by Organic Salts: Toward High-Performance Solution-Processed Organic Field-Effect Transistors. ACS Nano 2018, 12, 3938-3946.
- (6) Shi, K.; Zhang, F.; Di, C.-A.; Yan, T.-W.; Zou, Y.; Zhou, X.; Zhu, D.; Wang, J.-Y.; Pei, J. Toward High Performance n-Type Thermoelectric Materials by Rational Modification of BDPPV Backbones. *J. Am. Chem. Soc.* **2015**, *137*, 6979-6982.
- (7) Kiefer, D.; Giovannitti, A.; Sun, H.; Biskup, T.; Hofmann, A.; Koopmans, M.; Cendra, C.; Weber, S.; Anton Koster, L. J.; Olsson, E.; Rivnay, J.; Fabiano, S.; McCulloch, I.; Müller, C. Enhanced n-Doping Efficiency of a Naphthalenediimide-Based Copolymer through Polar Side Chains for Organic Thermoelectrics. *ACS Energy Lett.* **2018**, 278-285.
- (8) Shi, K.; Lu, Z.-Y.; Yu, Z.-D.; Liu, H.-Y.; Zou, Y.; Yang, C.-Y.; Dai, Y.-Z.; Lu, Y.; Wang, J.-Y.; Pei, J. A Novel Solution-Processable n-Dopant Based on 1,4-Dihydropyridine Motif for High Electrical Conductivity of Organic Semiconductors. *Adv. Electronic Mater.*, **2017**, *3*, 1700164.
- (9) Jung, I. H.; Hong, C. T.; Lee, U.-H.; Kang, Y. H.; Jang, K.-S.; Cho, S. Y. High Thermoelectric Power Factor of a Diketopyrrole-Based Low Bandgap Polymer via Finely Tuned Doping Engineering. *Sci. Rep.* **2017**, *7*, 44704.

- (10) Zhang, Q.; Sun, Y.; Jiao, F.; Zhang, J.; Xu, W.; Zhu, D. Effects of structural order in the pristine state on the thermoelectric power-factor of doped PBTTT films. *Synth. Met.* **2012**, *162*, 788-793.
- (11) Zhang, Q.; Sun, Y.; Xu, W.; Zhu, D. Thermoelectric energy from flexible P3HT films doped with a ferric salt of triflimide anions. *Energy Environ. Sci.* **2012**, *5*, 9639-9644.
- (12) Chen, L.; Liu, W.; Yan, Y.; Su, X.; Xiao, S.; Lu, X.; Uher, C.; Tang, X. Fine-tuning the solid-state ordering and thermoelectric performance of regionegular P3HT analogues by sequential oxygen-substitution of carbon atoms along the alkyl side chains. *J. Mater. Chem. C* **2019**, *7*, 2333-2344.
- (13) Glaudell, A. M.; Cochran, J. E.; Patel, S. N.; Chabinyc, M. L. Impact of the Doping Method on Conductivity and Thermopower in Semiconducting Polythiophenes. *Adv. Energy Mater.* **2015**, *5*, 1401072.
- (14) Hynynen, J.; Kiefer, D.; Yu, L.; Kroon, R.; Munir, R.; Amassian, A.; Kemerink, M.; Müller, C. Enhanced Electrical Conductivity of Molecularly p-Doped Poly(3-hexylthiophene) through Understanding the Correlation with Solid-State Order. *Macromolecules* **2017**, *50*, 8140-8148.
- (15) Lim, E.; Peterson, K. A.; Su, G. M.; Chabinyc, M. L. Thermoelectric Properties of Poly(3-hexylthiophene) (P3HT) Doped with 2,3,5,6-Tetrafluoro-7,7,8,8-tetracyanoquinodimethane (F4TCNQ) by Vapor-Phase Infiltration. *Chem. Mater.* **2018**, *30*, 998-1010.
- (16) Patel, S. N.; Glaudell, A. M.; Kiefer, D.; Chabinyc, M. L. Increasing the Thermoelectric Power Factor of a Semiconducting Polymer by Doping from the Vapor Phase. *ACS Macro Lett.* **2016**, 268-272.
- (17) Kang, K.; Watanabe, S.; Broch, K.; Sepe, A.; Brown, A.; Nasrallah, I.; Nikolka, M.; Fei, Z.; Heeney, M.; Matsumoto, D.; Marumoto, K.; Tanaka, H.; Kuroda, S.-i.; Sirringhaus, H. 2D

- coherent charge transport in highly ordered conducting polymers doped by solid state diffusion. *Nat. Mater.* **2016**, *15*, 896-902.
- (18) Scholes, D. T.; Hawks, S. A.; Yee, P. Y.; Wu, H.; Lindemuth, J. R.; Tolbert, S. H.; Schwartz, B. J. Overcoming Film Quality Issues for Conjugated Polymers Doped with F4TCNQ by Solution Sequential Processing: Hall Effect, Structural, and Optical Measurements. *J. Phys. Chem. Lett.* **2015**, *6*, 4786-4793.
- (19) Scholes, D. T.; Yee, P. Y.; Lindemuth, J. R.; Kang, H.; Onorato, J.; Ghosh, R.; Luscombe, C. K.; Spano, F. C.; Tolbert, S. H.; Schwartz, B. J. The Effects of Crystallinity on Charge Transport and the Structure of Sequentially Processed F4TCNQ-Doped Conjugated Polymer Films. *Adv. Funct. Mater.*, **2017**, *27*, 1702654.
- (20) Ferreira, A. S.; Aguirre, J. C.; Subramaniyan, S.; Jenekhe, S. A.; Tolbert, S. H.; Schwartz, B. J. Understanding How Polymer Properties Control OPV Device Performance: Regioregularity, Swelling, and Morphology Optimization Using Random Poly(3-butylthiophene-co-3-octylthiophene) Polymers. *J. Phys. Chem. C* **2016**, *120*, 22115-22125.
- (21) Perry, E. E.; Chiu, C.-Y.; Moudgil, K.; Schlitz, R. A.; Takacs, C. J.; O'Hara, K. A.; Labram, J. G.; Glaudell, A. M.; Sherman, J. B.; Barlow, S.; Hawker, C. J.; Marder, S. R.; Chabinyc, M. L. High Conductivity in a Nonplanar n-Doped Ambipolar Semiconducting Polymer. *Chem. Mater.* **2017**, *29*, 9742-9750.
- (22) Scholes, D. T.; Yee, P. Y.; McKeown, G. R.; Li, S.; Kang, H.; Lindemuth, J. R.; Xia, X.; King, S. C.; Seferos, D. S.; Tolbert, S. H.; Schwartz, B. J. Designing Conjugated Polymers for Molecular Doping: The Roles of Crystallinity, Swelling, and Conductivity in Sequentially-Doped Selenophene-Based Copolymers. *Chem. Mater.* **2018**, *31*, 73-82.
- (23) Zuo, G.; Liu, X.; Fahlman, M.; Kemerink, M. High Seebeck Coefficient in Mixtures of

- Conjugated Polymers. Adv. Funct. Mater., 2018, 28, 1703280.
- (24) Li, H.; DeCoster, M. E.; Ireland, R. M.; Song, J.; Hopkins, P. E.; Katz, H. E. Modification of the Poly(bisdodecylquaterthiophene) Structure for High and Predominantly Nonionic Conductivity with Matched Dopants. *J. Am. Chem. Soc.* **2017**, *139*, 11149-11157.
- (25) Wang, S.; Fazzi, D.; Puttisong, Y.; Jafari, M. J.; Chen, Z.; Ederth, T.; Andreasen, J. W.; Chen, W. M.; Facchetti, A.; Fabiano, S. Effect of Backbone Regiochemistry on Conductivity, Charge Density, and Polaron Structure of n-Doped Donor–Acceptor Polymers. *Chem. Mater.* **2019**, *31*, 3395-3406.
- (26) Naab, B. D.; Gu, X.; Kurosawa, T.; To, J. W. F.; Salleo, A.; Bao, Z. Role of Polymer Structure on the Conductivity of N-Doped Polymers. *Adv. Electronic Mater.* **2016**, *2*, 1600004.
- (27) Kroon, R.; Kiefer, D.; Stegerer, D.; Yu, L.; Sommer, M.; Müller, C. Polar Side Chains Enhance Processability, Electrical Conductivity, and Thermal Stability of a Molecularly p-Doped Polythiophene. *Adv. Mater.* **2017**, 1700930.
- (28) Liu, J.; Qiu, L.; Alessandri, R.; Qiu, X.; Portale, G.; Dong, J.; Talsma, W.; Ye, G.; Sengrian, A. A.; Souza, P. C. T.; Loi, M. A.; Chiechi, R. C.; Marrink, S. J.; Hummelen, J. C.; Koster, L. J. A. Enhancing Molecular n-Type Doping of Donor-Acceptor Copolymers by Tailoring Side Chains. *Adv. Mater.* **2018**, *30*, 1704630.
- (29) Mazaheripour, A.; Thomas, E. M.; Segalman, R. A.; Chabinyc, M. L. Nonaggregating Doped Polymers Based on Poly(3,4-Propylenedioxythiophene). *Macromolecules* **2019**, *52*, 2203-2213.
- (30) Suh, E. H.; Jeong, Y. J.; Oh, J. G.; Lee, K.; Jung, J.; Kang, Y. S.; Jang, J. Doping of donor-acceptor polymers with long side chains via solution mixing for advancing thermoelectric properties. *Nano Energy* **2019**, *58*, 585-595.

- (31) Vijayakumar, V.; Zaborova, E.; Biniek, L.; Zeng, H.; Herrmann, L.; Carvalho, A.; Boyron, O.; Leclerc, N.; Brinkmann, M. Effect of Alkyl Side Chain Length on Doping Kinetics, Thermopower, and Charge Transport Properties in Highly Oriented F4TCNQ-Doped PBTTT Films. *ACS Appl. Mater. Interf.* **2019**, *11*, 4942-4953.
- (32) Li, J.; Zhang, G.; Holm, D. M.; Jacobs, I. E.; Yin, B.; Stroeve, P.; Mascal, M.; Moulé, A. J. Introducing Solubility Control for Improved Organic P-Type Dopants. *Chem. Mater.* **2015**, *27*, 5765-5774.
- (33) Saska, J.; Gonel, G.; Bedolla-Valdez, Z. I.; Aronow, S. D.; Shevchenko, N. E.; Dudnik, A. S.; Moulé, A. J.; Mascal, M. A Freely Soluble, High Electron Affinity Molecular Dopant for Solution Processing of Organic Semiconductors. *Chem. Mater.* **2019**, *31*, 1500-1506.
- (34) Jacobs, I. E.; Moulé, A. J. Controlling Molecular Doping in Organic Semiconductors. *Adv. Mater.* **2017**, *29*, 1703063.
- (35) Un, H.-I.; Gregory, S. A.; Mohapatra, S. K.; Xiong, M.; Longhi, E.; Lu, Y.; Rigin, S.; Jhulki, S.; Yang, C.-Y.; Timofeeva, T. V.; Wang, J.-Y.; Yee, S. K.; Barlow, S.; Marder, S. R.; Pei, J. Understanding the Effects of Molecular Dopant on n-Type Organic Thermoelectric Properties. *Adv. Energy Mater.* **2019**, *9*, 1900817.
- (36) Aubry, T. J.; Axtell, J. C.; Basile, V. M.; Winchell, K. J.; Lindemuth, J. R.; Porter, T. M.; Liu, J.-Y.; Alexandrova, A. N.; Kubiak, C. P.; Tolbert, S. H.; Spokoyny, A. M.; Schwartz, B. J. Dodecaborane-Based Dopants Designed to Shield Anion Electrostatics Lead to Increased Carrier Mobility in a Doped Conjugated Polymer. *Adv. Mater.* **2019**, *31*, 1805647.
- (37) Liang, Z.; Zhang, Y.; Souri, M.; Luo, X.; Boehm, Alex M.; Li, R.; Zhang, Y.; Wang, T.; Kim, D.-Y.; Mei, J.; Marder, S. R.; Graham, K. R. Influence of dopant size and electron affinity on the

- electrical conductivity and thermoelectric properties of a series of conjugated polymers. *J. Mater. Chem. A* **2018**, *6*, 16495-16505.
- (38) McCulloch, I.; Heeney, M.; Bailey, C.; Genevicius, K.; MacDonald, I.; Shkunov, M.; Sparrowe, D.; Tierney, S.; Wagner, R.; Zhang, W.; Chabinyc, M. L.; Kline, R. J.; McGehee, M. D.; Toney, M. F. Liquid-crystalline semiconducting polymers with high charge-carrier mobility. *Nat. Mater.* **2006**, *5*, 328-333.
- (39) Li, H.; Dailey, J.; Kale, T.; Besar, K.; Koehler, K.; Katz, H. E. Sensitive and Selective NO2 Sensing Based on Alkyl- and Alkylthio-Thiophene Polymer Conductance and Conductance Ratio Changes from Differential Chemical Doping. *ACS Appl. Mater. Interf.* **2017**, *9*, 20501-20507.
- (40) Pingel, P.; Neher, D. Comprehensive picture of p-type doping of P3HT with the molecular acceptor F4TCNQ. *Phys. Rev. B* **2013**, *87*, 115209.
- (41) Méndez, H.; Heimel, G.; Winkler, S.; Frisch, J.; Opitz, A.; Sauer, K.; Wegner, B.; Oehzelt, M.; Röthel, C.; Duhm, S.; Többens, D.; Koch, N.; Salzmann, I. Charge-transfer crystallites as molecular electrical dopants. *Nat. Commun.* **2015**, *6*, 8560.
- (42) Li, H.; Plunkett, E.; Cai, Z.; Qiu, B.; Wei, T.; Chen, H.; Thon, S. M.; Reich, D. H.; Chen, L.; Katz, H. E. Dopant-Dependent Increase in Seebeck Coefficient and Electrical Conductivity in Blended Polymers with Offset Carrier Energies. *Adv. Electronic Mater.* **2019**, 1800618.
- (43) Hopkins, P. E. Thermal Transport across Solid Interfaces with Nanoscale Imperfections: Effects of Roughness, Disorder, Dislocations, and Bonding on Thermal Boundary Conductance. *ISRN Mech. Engin.* **2013**, 1-19.
- (44) Hopkins, P. E.; Serrano, J. R.; Phinney, L. M.; Kearney, S. P.; Grasser, T. W.; Harris, C. T. Criteria for Cross-Plane Dominated Thermal Transport in Multilayer Thin Film Systems During Modulated Laser Heating. *J. Heat Transfer* **2010**, *132*, 081302-081310.

- (45) Gregory, S. A.; Menon, A. K.; Ye, S.; Seferos, D. S.; Reynolds, J. R.; Yee, S. K. Effect of Heteroatom and Doping on the Thermoelectric Properties of Poly(3-alkylchalcogenophenes). *Adv. Energy Mater.* **2018**, *8*, 1802419.
- (46) Mott, N. F.; Davis, E. A. Electronic Processes in Non-Crystalline Materials, 2nd Ed., Oxford University Press, Oxford 2012.
- (47) Mott, N. F. Conduction in glasses containing transition metal ions. *J. Non-Cryst. Solids* **1968**, *1*, 1-17.
- (48) Cutler, M.; Mott, N. F. Observation of Anderson Localization in an Electron Gas. *Phys. Rev.* **1969**, *181*, 1336-1340.
- (49) Loponen, M. T.; Taka, T.; Laakso, J.; Väkiparta, K.; Suuronen, K.; Valkeinen, P.; Österholm, J. E. Doping and dedoping processes in poly (3-alkylthiophenes). *Synth. Met.* **1991**, *41*, 479-484. (50) Cochran, J. E.; Junk, M. J. N.; Glaudell, A. M.; Miller, P. L.; Cowart, J. S.; Toney, M. F.; Hawker, C. J.; Chmelka, B. F.; Chabinyc, M. L. Molecular Interactions and Ordering in Electrically Doped Polymers: Blends of PBTTT and F4TCNQ. *Macromolecules* **2014**, *47*, 6836-6846.

## for Table of Contents use only

